 doi:10.20944/preprints201910.0344.v1

Article

Synthesis and Characterization of TiO_2/Natural Fiber from Banana Fruit Bunch Waste for Removal of Rhodamine-B in Aqueous Solution

Allwar Allwar

Department of Chemistry, Faculty Mathematics and Natural Sciences, Universitas Islam Indonesia (UII), Yogyakarta, 55584, Indonesia

* Correspondence: allwar@uii.ac.id; Tel.: +628112551896

Abstract: Indonesia is one of the largest banana producing countries in the world remaining abundance solid waste of banana fruit bunch. The banana fruit bunch contains high natural fibers which were obtained by an impregnation process using potassium hydroxide (KOH) and followed by a carbonization process under steam at 250°C for 5 h. The nanomaterial of TiO_2/fibre was prepared by a hydrothermal process at 200°C for 4 h. Surface morphology proved that the TiO_2 was loaded into the fibre by an increasing roughness of the surface and irregular size of porosity. The development of amorphous to crystalline phase of TiO_2/fibre was clearly observed. The effectiveness of TiO_2/fibre for removal of rhodamine B was investigated from different parameters of adsorptions in aqueous solution. The equilibrium adsorptions show that the Langmuir and Freundlich isotherm exhibited the best correlation coefficient ($R^2 > 0.94$) relating to the chemisorption and physisorption interaction in the adsorption process. Kinetic models were well described by the pseudo-first and second-order with the best correlation coefficient ($R^2 > 0.99$). These results indicate that nanomaterial TiO_2/fibre can be used as an effective adsorbent for removal of rhodamine B in aqueous solution.

Keywords: banana empty fruit bunch; TiO_2/fibre; adsorption; rhodamine B; isotherm and kinetic adsorptions

1. Introduction

The exploration of population growth has led to an increase in modern industry. The increasing utilization of dye in the industry has become the global issues in environmental problem. The dye pollutions produced by industrial activities such as textiles, paints, printing are found in many streams of water [1]. The pollutions consist of complex aromatic structure with highly hazardous materials that can lead to destruction and even death of living things and humans [2]. Rhodamine B is one of basic dyes used in many applications in industries. Although the utilization of rhodamine B was intensively controlled, their effects on the environment are still controversial. It is because of the difficulty to detrmine their properties separately. Various methods have been applied to reduce the level of dye pollution in water and recovery them for example as precipitation, electrochemical reduction and reverse osmosis. Most of them are strongly considered due to high cost process and recurring expenses, which are not appropriate for the waste treatment in the small-scale industries. The alternative method with the utilization of the adsorbents have been intensively studied and widely used for the separation and purification in the aqueous solution. There have many types of adsorbents such as activated carbon, composite, fibre and metal oxide/fibre that are used for the removal of dye contaminants [3]. The by-products having natural fibre such as oil palm empty fruit bunch, banana fruit bunch, sugar cane bagasse, etc. have been considered as a good alternative raw material due to the co-friendly and renewable nature [4]. Composite of metal oxide coated with natural fibre offer various advantages such as low energy-consumption, low density, biodegradable, low-cost materials and available in large quantity.

 doi:10.20944/preprints201910.0344.v1

Indonesia is one of the largest banana producers in the world and experiencing a fast development in increasing production. The production of banana is a continuously increasing annually, which is followed by the producing of large quantity of solid wastes such as empty fruit bunch. Biochemical and ultimate analysis proved that banana fruit bunch consists of fibre (8.8%), hemicellulose (21.23%), lignin (19.06%) and carbon (41.75%), hydrogen (5.10%), oxygen (51.73%), nitrogen (1.23%) [5]. These data revealed that banana fruit bunch is a good alternative as the raw material for production of fibre and is interesting to explore as an adsorbent for removal or recovery of dyes from wastewater [6–8].

Recently, utilizations of by-product with high fibre have a great progress in research and its application as an adsorbent for developing sustainable and environmentally friendly resources [9,10]. However, natural fibres have some weaknesses as adsorbent such as the unpredictable mechanism and barrier properties. The improvement of the performance of an adsorbent prepared from the natural fibre can be achieved by the modification process using metal oxide. The natural fibre is a polymeric composite which can be explored as matrixes to provide the particular the tensile strength, flexural strength and elongation at breaks. Combinations with suitable ratio of natural fibre and metal oxide have been intensively studied to form the composite metal oxide/fibre and used as an adsorbent for removal of dyes [11,12].

The aim of the presence work is to obtain the features of nanomaterial composite of TiO_2/fibre from banana fruit bunch. The characterization of TiO_2/fibre was carried out by SEM, XRD, FTIR and SAA. The effectiveness of composite was investigated for removal of rhodamine B from aqueous solution at different adsorption parameters involving solution pH, concentration, contact time and adsorbent dose. Experimental adsorptions were carried out by batch methods at room temperature. Adsorption equilibriums were investigated by the Langmuir and Freundlich isotherm and kinetics adsorption models.

2. Materials and methods

2.1. Material

Banana fruit bunch was collected from the banana seller in Yogyakarta, Indonesia. The chemicals such as rhodamine B as shown Figure. 1, potassium hydroxide (KOH), hydrochloric acid (HCl), nitric acid (HNO_3) and ethanol were obtained in analytical grade from Merck and used without further purification.

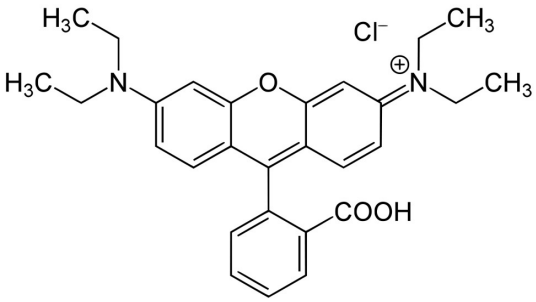

Figure 1. Rhodamine B structure.

2.2. Preparation of natural fibre

Natural fibre was prepared from banana fruit bunch waste, collected from banana seller by carbonization process under steam and chemical activation. The raw material was initially cut in to small pieces in the range of 0.5-1.0 cm, washed with distilled water and then dried in an oven at 110°C for 24 h. The dried sample was soaked in 20% KOH solution and refluxed at 85°C for 6 h. It was washed with distilled water and neutralized with 2 M nitric acid solution to pH 6-7. The sample was

 doi:10.20944/preprints201910.0344.v1

carbonized under the steam at 250°C for 5 h and continued to dry in an oven at 110°C for 24 h. Resulted fibre was stored for further analysis.

2.3. Preparation of TiO_2/fibre

The fibre was weighted 100 g and added with 20 g of commercial nanomaterial of TiO_2 in a beaker glass. The mixture was immersed in solution of de-ionized water and ethanol with ratio 1:1 while vigorously stirred for 1 h to homogeneous solution. It was transferred in a hydrothermal reactor, and then nitrogen gas was flowed in to reactor. The reactor was placed into graphite furnace and slowly heated up to 200°C for 4 h. After cooling down, the resulted TiO_2/fibre was stored in desiccator for further analysis.

2.4. Adsorption study

Rhodamine B is a basic dye consisting of heterocyclic aromatic chemical moiety. The stock solution of 1000 ppm dye was quantitatively prepared by dissolving 1 g of rhodamie B in 1000 ml of distilled water. The experimental adsorptions were conducted with different parameters involving solution pH, contact time, concentration and dosage of adsorbent. The amount of adsorption was determined by UV-Visible spectrophotometer at 555 nm.

2.5. Characterization of TiO_2/fibre

Characterizations of the fibre and composite TiO_2/fibre were conducted to observe their physical and chemical properties. Surface morphology was determined by the Scanning electron micrograph (SEM). The crystallite phase and crystallographic structure were investigated by the X-Ray diffraction (XRD). Surface functional groups were studied by the Fourier transform infrared (FTIR) using potassium bromide (KBr) to perform the thin pellet.

2.6. Batch adsorption Study

The effectiveness of TiO_2/fibre was evaluated on the removal of rhodamine B using batch method at room temperature. The adsorption capacity was affected by the various pH solutions, initial concentration, composite dosage and contact time. The concentration of the dye was analysed using a UV-Vis spectrophotometer at 555 nm. The adsorption capacity by a unit mass of the adsorption percentage (% *R*) and the amount of the equilibrium adsorption, *qe* (mg/g) were measured using the following the equation (1) and (2), respectively.

$$\% R = \frac{Co - Ct}{C_o} x\ 100 \quad (1)$$

$$q_e = \frac{Co - Ce}{m} x\ V \quad (2)$$

where *Co* (mg/L) is the initial concentration; *Ce* (mg/L) is the concentration absorbed at equilibrium; *Ct* (mg/L) is the concentration at any time; m (g) is the mass of composite and V is the volume.

3. Results and discussion

3.1. Collecting, Processing and Characterization of loaded fibre

Photographic pictures of the banana fruit bunch, fibre and TiO_2/fibre were shown in Figure 2. The brown color of fiber was modified with nitric acid to remove the lignin and other impurities in the fibre. The addition of nanomaterial of TiO_2 to the fibers was successfully changed the color from dark brow to grey as a result of loaded TiO_2 to the fiber materials.

Preprints (www.preprints.org) | NOT PEER-REVIEWED | Posted: 30 October 2019 doi:10.20944/preprints201910.0344.v1

Figure 2. Photographic pictures: (a) banana fruit bunch; (b) natural fibre; (c) TiO_2/fibre.

3.2. Determination of surface morphology

Overviews of surface morphology for the fibre and TiO_2/fibre composite are shown in Figure 3. An alkaline and acidic treatments with potassium hydroxide and nitric acid played important rule for the acceleration of the removal of lignin, hemicellulose and other impurities attached on the surface of the fibre including the formation of pores and functional groups [13]. The smooth surface with a cross-section structure is clearly shown as natural fibre as displayed in Figure 3(a). The surface morphology of the fibre was clearly observed with an irregular form due to the chemical activation process [14]. The attachment of TiO_2 on the fibre was confirmed by the SEM as shown in Figure 3(b). The surface morphology of TiO_2/fibre was clearly observed as an increase with the roughness of the surface with a cross-sectional irregular form. This result showed that the surface was partially loaded by the TiO_2 as a coating process of TiO_2/fibre.

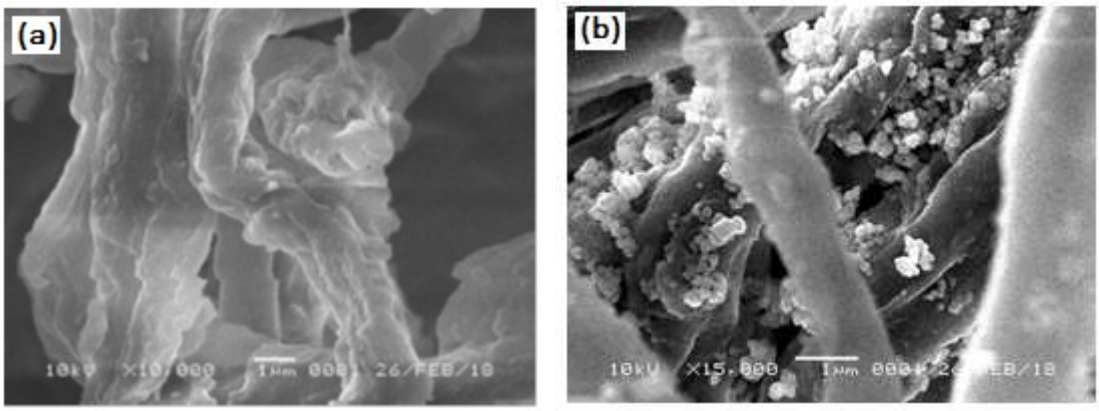

Figure 3. Scanning electron micrographs: (a) natural fibre materials; (b) TiO_2/fibre.

3.3. Determination of functional groups of the fibre

Infrared spectroscopy gives one of the useful information for investigating the structure and functional groups. The FTIR spectra of the fibre and TiO_2/fibre are obtained from the wave number in the range of 4000-400 cm^{-1} as shown in Figure 4. The results show that the FTIR spectra for the fibre (Figure 4a) and TiO_2/fibre (Figure 4b) are no significant differences in the wave number. The strong bands at 3336 and 3334 cm^{-1} are assigned to strong hydrogen-bonded OH stretching. The intensity of the fibre band shows higher than that of the TiO_2/fibre due to the replacement of O-H to Ti-O bond. The crystallinity index of the TiO_2/fibre proved that there was a degradated amorphous structure by reducing amount of hydrogen bonding and replacing with Ti-O bonds. The strong bands found at around 2906 and 2896 cm^{-1} are attributed to the symmetrical stretching of aliphatic C-H groups. The bands around 1633 and 1596 cm^{-1} are related to OH stretching vibration of adsorbed water [15]. The

 doi:10.20944/preprints201910.0344.v1

peak at 1315 cm^{-1} related to C=O and C-O of the carboxylic group which is the indicative of oxygen-containing functional groups. The band at around 1159 and 1160 cm^{-1} are assigned to the symmetrical stretching of C-O-C groups. The bands found at 1032-1056 cm^{-1} are assigned to C-C, C-OH and C-H ring and side group vibration. The presences of C-O-C, C-C-O and C-C-H deformation and stretching on the fibre are attributed to band 896 cm^{-1} the; C-OH out-of-plane at band 550 cm^{-1}. The presence of additional peak at band 450 cm^{-1} on the TiO_2/fibre spectra is assigned to the Ti-O bond.

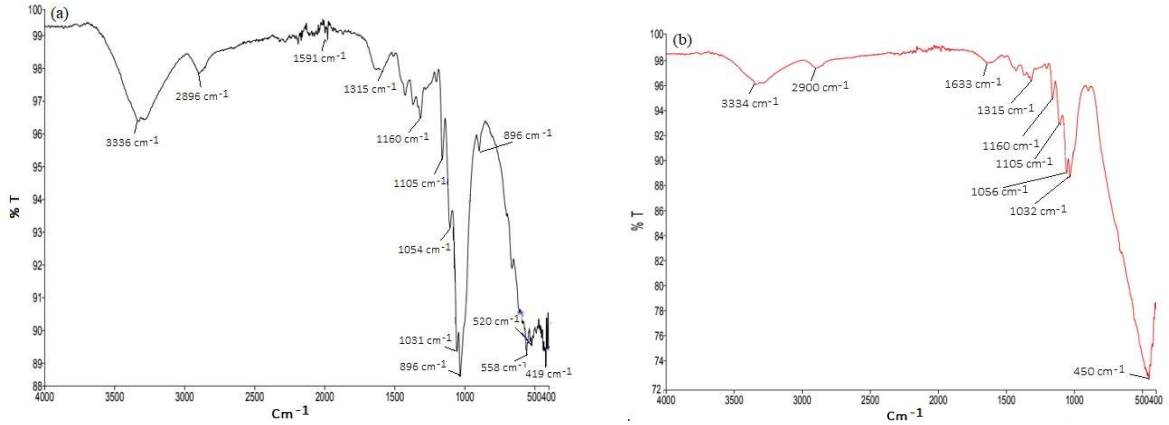

Figure 4. FTIR spectra (a) natural fibre and (b) TiO_2/fibre.

3.4. Determination of XRD

The X-ray diffraction patterns of the fibre and nanomaterial of TiO_2/fibre were investigated for studying the molecular structure and crystalline phase as shown in Figure 5. The data was taken for the 2θ ranging from 10° to 85°. The diffraction patterns of the fibre exhibited two broad diffraction peaks at around 2θ = 15.8° and 23.2° indicating predominantly amorphous structures. The diffraction patterns of TiO_2/fibre composite (based on the high-intensity crystal peaks) are located at around 2θ = 25.8°, 38.3°, 48.5°, 54.3°, 55.5, 63.0 ° and 75.5 ° that are indexed as (101), (004), (200), (105), (211), (204) and (215), respectively. These results clearly show anatase crystalline phase of TiO_2 which was confirmed with the JCPDS card no 21-1272 [16–18].

Preprints (www.preprints.org) | NOT PEER-REVIEWED | Posted: 30 October 2019 doi:10.20944/preprints201910.0344.v1

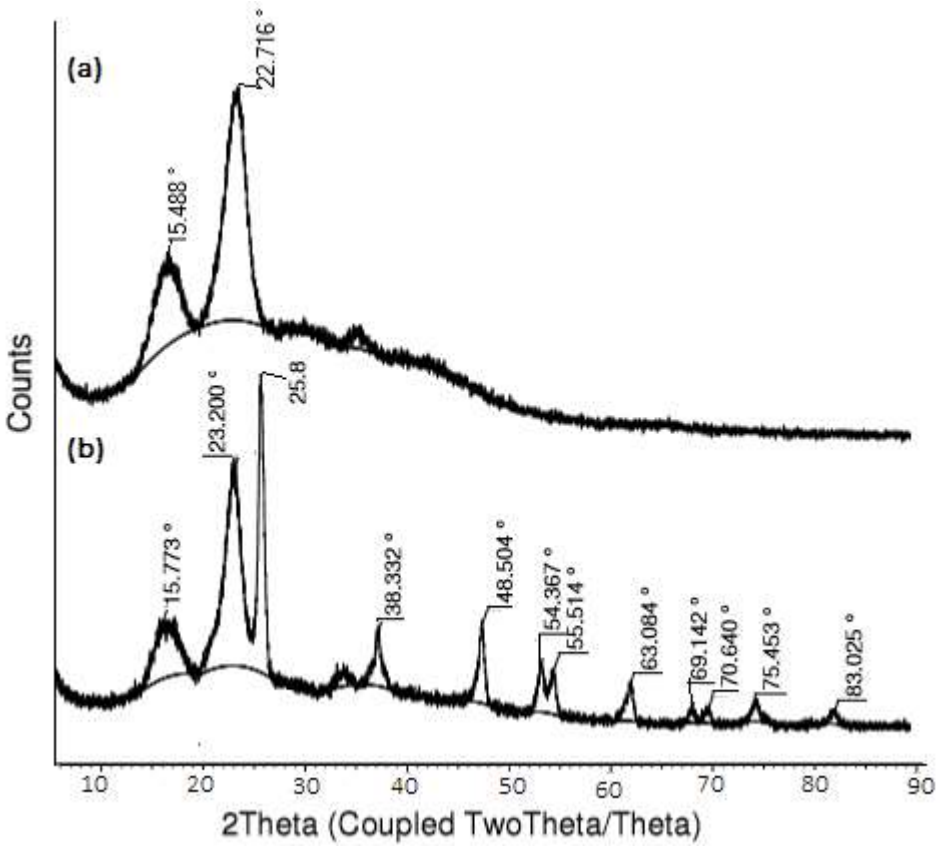

Figure 5. X-ray diffraction patterns: (a) fibre; (b) TiO_2/fibre.

3.5. The effect of pH

Previous studies reported that the initial pH is an important factor for controlling the adsorption process by the formation of complexion. The effect of pH solution initiated to the change of the charge on composite surface with the change of pH value. The rates of adsorption are performed at different pH ranging from pH 2 to 10. The effect of pH on the TiO_2/fibre for the removal of rhodamine B is shown in Figure 6(a). The amount of adsorption increases from pH 2 to 4 and then slightly decreases from pH 4 to pH 10. The maximum sorption is obtained at the pH 4 which was used for all experiments. The increase the plot at pH < 4 could be caused by the formation of the negative charges on the composite surface and the release of proton. Therefore, the zwitterion form of adsorbate is affected by the presence of proton by competing of ions from $-N^+$ and $-COO^-$. Consequently, the dye becomes lower aggregation by producing positive charges. The electrostatic interaction between the negative charges from the surface of composite and the positive charges from the adsorbates accelerated the formation of complexation. At pH > 4, the zwitterion of rhodamine B may increase the aggregation to form a bigger structure and produce negative charges, and then the ionic rhodamine B repelled the ionic composite. This result showed that the decrease of the plot starting from pH 4 to 6. [19].

3.6. Effect of contact times

The effects of the contact time on rhodamine B adsorption are shown in Figure 6(b). The adsorption rapidly increases at the initial period of contact time to 30 min which is followed with the maximum adsorption. It is because a strong attractive force occurred between the TiO_2/fibre composite and the rhodamine B molecules. At the contact time higher than 30 min, the adsorption of the rhodamine B slightly decreases to 45 min and then increases to the end of reaction of 60 min. There is indicative of a weaker attractive force at 45 min indicating of nearly saturated condition. As result, the rhodamine B molecules were adsorbed by the adsorbent and leaved the aqueous solution.

Preprints (www.preprints.org) | NOT PEER-REVIEWED | Posted: 30 October 2019 doi:10.20944/preprints201910.0344.v1

191 The extensions of the contact time have increased the interaction between the rhodamine B molecules
192 and the TiO_2/fibre composite followed by an increasing the removal of rhodamine B.

193 *3.7. Effect of adsorbent dosage*

194 The effects of the adsorbent dosage on the adsorption of rhodamine B onto TiO_2/fibre are shown
195 in Figure 6(c). The capacity adsorption increases from the 0.5 to 1.0 g and then gradually decreases
196 to the maximum adsorbent dosage of 2 g. The increase of adsorption of the rhodamine B onto the
197 TiO_2/fibre composite may be due to the increase of the number of surface area and the availability
198 more pores of the surface of composite. This reason may support to rapid transportation by strongly
199 attractive force between rhodamine B molecules from aqueous solution and active sites of composite.
200 However, the decrease of adsorption capacity is due to the reduce of the equilibrium concentration
201 of rhodamine B in aqueous solution with increasing of the adsorbent dosage.

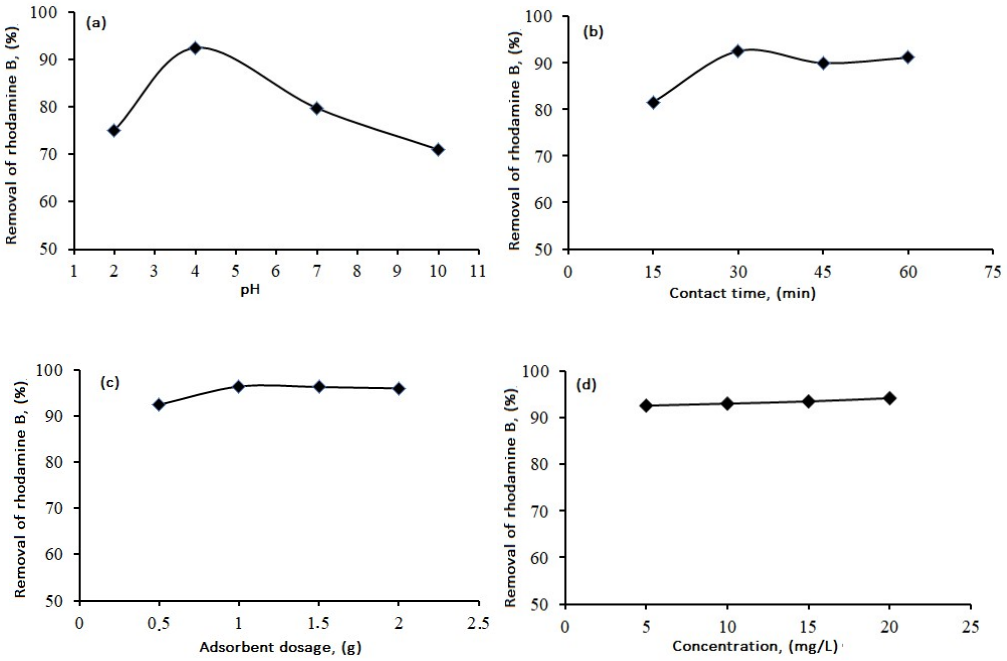

202

203

204 **Figure 6.** Removal of rhodamine-B onto TiO_2/fibre affected by: (a) pH solution; (b) contact time; (c)
205 adsorbent dosage; (d) concentration.

206 *3.8. Effect of concentration*

207 The effects of the concentration on the adsorption of rhodamine B onto TiO_2/fibre composite are
208 illustrated in Figure 6(d). The experiments of the adsorptions are carried out at the different
209 concentrations ranging from 5 to 20 mg/L. At the initial concentration, the percentage of the
210 adsorption increases from 5 to 10 mg/L with the maximum adsorption at 10 mg/L. These features
211 have been noted that with increasing concentration, more rhodamine B molecules can be filled to the
212 vacant pores with the strong attractive force from TiO_2/fibre composite. However, at the
213 concentration is higher than 10 mg/L, the percentage adsorption slightly decreased. It assumed due
214 to the saturation of the pores of the adsorbent.

215 *3.9. Adsorption isotherm study*

216 In this study, two isotherm models, the Langmuir and Freundlich isotherm are conducted to
217 investigate the adsorption of rhodamine B onto TiO_2/fibre. The Langmuir isotherm generally
218 describes the specific monolayer with the homogeneous sites on the surface which is expressed as
219 Eq. 1.

Preprints (www.preprints.org) | NOT PEER-REVIEWED | Posted: 30 October 2019 doi:10.20944/preprints201910.0344.v1

$$\frac{C_e}{q_e} = \frac{1}{q_m K_L} + \frac{C_e}{q_m} \quad (1)$$

where q_e (mg/g) is the amount of rhodamine B adsorbed per unit mass of composite at the equilibrium, C_e (mg/L) is the equilibrium concentration, The Q_m (mg/g) is the maximum amount of rhodamine B adsorbed, K_L (L/mg) is the Langmuir constant related the adsorption energy. The value of q_m is calculated from the slope ($1/q_m$) and intercept ($1/q_m K_L$) using the linier plot of C_e/q_e) versus C_e.

The Freundlich isotherm generally describes the adsorption process that occurs on the heterogeneous surface. The Freundlich equation is expressed as eq.2.

$$\log q_e = \frac{1}{n} \log C_e + \log K_F \quad (2)$$

where K_F is the Freundlich constant which related to distribution coefficient and indicative of the adsorption capacity and n is indicative of adsorption intensity. Their values were calculated from the intercept (log K_F) and slop ($1/n$) based on the linier plot of loq q_e versus log C_e.

It is very important to obtain the appropriate correlation coefficient (R^2) for the adsorption equilibrium. The Langmuir and Freundlich isotherm plots are shown in Figure 7. The equilibrium adsorptions were obtained from the result of different concentrations. The Langmuir isotherm decrease with increasing of the equilibrium concentration with the value of correlation coefficient, R^2 = 0.9459. However, the Freundlich isotherm has the higher correlation coefficient, R^2 of 0.9942. The observation of R^2 values are obtained between 0 and 1. If the value of R^2 is close to the unity, it implies that the adsorption is desirably adsorbed on the adsorbent. Furthermore, the value of correlation coefficient (R^2) for the Langmuir and Freundlich isotherm are shown in Table 1. These result shows that the interactions of rhodamine B and TiO_2/fibre could be occurred by the physisorption and chemisorption process.

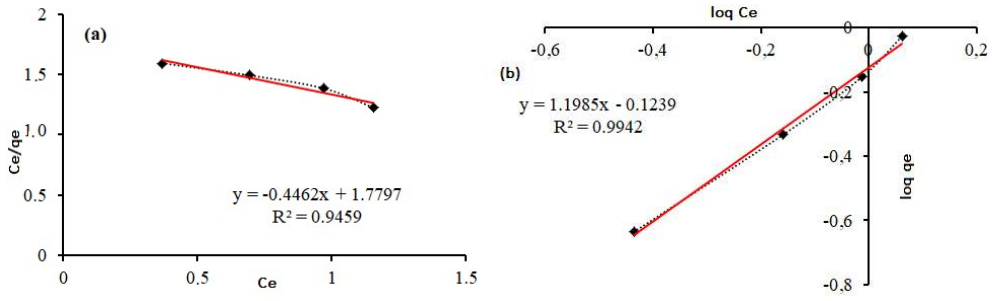

Figure 7. Adsorption equilibrium models: (a) the Langmuir isotherm; (b) Freundlich isotherm.

Table 1. The Langmuir and Freundlich isotherms for the adsorption of rhodamine B onto TiO_2/fibre.

Adsorbate	Langmuir Isotherm				Freundlich Isotherm		
	qe (mg/g)	K_L (L/mg)	R^2	R_L	K_F	n	R^2
Rh-B	-2.24	- 0.26	0.95	1.11	0.75	0.83	0.99

3.10. Adsorption kinetics

Two models for the kinetics, the pseudo-first-order and pseudo-second-order are used to study the mechanism of rhodamine B removal onto TiO_2/fibre.

Preprints (www.preprints.org) | NOT PEER-REVIEWED | Posted: 30 October 2019 doi:10.20944/preprints201910.0344.v1

a. The first-pseudo-order can be expressed as the following eq. 3.

$$\log (q_e - q_t) = \log q_e - \frac{k_1}{2.303} t \quad (3)$$

where q_e and q_t are the amounts of rhodamine B adsorbed (mg/g) at the equilibrium and at any time, t (min), respectively. k_1 (1/min) is rate constant of the adsorption that can be obtained from the plot of ln(qe-qt) versus t.

b. The second-pseudo-order can be expressed as the following eq.4.

$$\frac{t}{q_t} = \frac{1}{k_2 q_e^2} + \frac{1}{q_t} t \quad (4)$$

where k_2 is the rate constant (g/mg.min) calculated from the linier plot of t versus t/q_t and related with the values of qt and the intercept.

Removal of rhodamine B onto TiO_2/fibre was evaluated from the plots of pseudo-first-order and second-order as shown in Figure 8. The kinetic data were calculated from the different contact time data using the plots of log (qe-qt) versus t and t/qt versus t, respectively. The results showed that the pseudo-first-order and second-order are applicable with the best linier relationship. The calculation of the pseudo-first and second-order for different temperatures were shown in Table 2. It is important to note that both kinetic models have high correlation coefficient ($R^2 > 0.99$). These results indicated that the reaction process of rhodamine B removal onto TiO_2/fibre could be more inclined toward the physisorption and chemisorption.

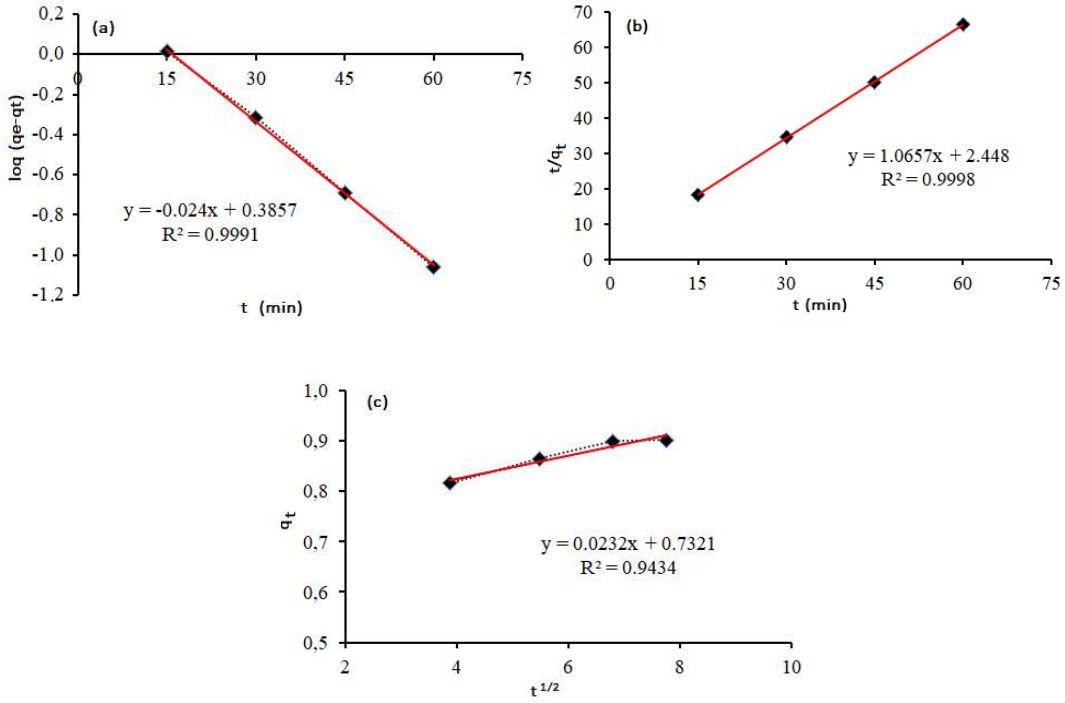

Figure 8. Kinetic modeling for adsorption process: (a) pseudo-first-order; (B) pseudo-second–order; (c) and intra-diffusion particle.

Table 2. Kinetic modeling of removal rhodamine B onto TiO_2/fibre.

Pseudo-first-order			Pseudo-second-order			Intra-particle-diffusion		
q_e (mg/g)	k_1 (1/min)	R^2	q_t (mg/g)	k_2 (g/mg.min)	R^2	K_d (mg/g $min^{1/2}$)	R^2	C
2.43	-0.06	0.99	0.94	0.46	0.99	0.02	0.94	0.73

c. Intro-particle-diffusion of rhodamine B

The mechanism of adsorption process can be carried out by several steps involving the transport of adsorbate from aqueous phase to the surface of adsorbent and followed by molecules into the interior of the porous materials [20]. The adsorption process can be described in two ways: (a) the bulk solution transport, the adsorbate diffuse from aqueous solution to the boundary layer surrounding with the adsorbents; (b) the film diffusion: the adsorbate diffuse through the liquid film surrounding with the adsorbents. In this study, the removal of rhodamine B onto porous TiO_2/fibre was also controlled by the intra-particle diffusion models that can be expressed as the following eq. 5.

$$q_t = K_d\, t^{1/2} + C \quad (5)$$

where q_t (mg/g) is the amount of concentration adsorbed at any time, t (min), K_d (mg/g $min^{1/2}$) is the rate constant of the intra-particle diffusion and C (mg/g) is the intercept representing the thickness of boundary layer; the larger the value of C, the greater the boundary layer thickness [21]. According to this equation, the curve of qt versus $t^{1/2}$ should be linier, and then the intra-particle diffusion is the rate controlling step. However, if the line is not passing through the origin, it is indicative of the degree of boundary layer control, and the intra-particle diffusion is not the only rate limiting step [22].

Further analysis was carried out from kinetic data for investigating of adsorption mechanism. Intra-particle diffusion of composite was shown in Figure 7(c). It could be suggested that rhodamine B transport onto the composite was controlled by the intra-particle diffusion which was shown by the best linearity of the correlation coefficient (R^2 = 9.9434). However, the line does not pass through the origin. It proved that the intra-particle diffusing is not rate-controlling step for the adsorption in the system.

4. Conclusion

Nanomaterial of TiO_2/fibre was successfully obtained from the mixture of natural fibre from banana fruit bunch and titanium oxide. The characterization showed that surface morphology exhibited a strong attractive force between fibre and titanium oxide with an increase the roughness on the surface. The X-Ray diffraction (XRD), Fourier transform infrared (FTIR) and Scanning electron micrograph and energy-dispersive X-Ray spectroscopy (SEM-EDX) were successfully used to investigate the molecular structure of TiO_2/fibre. The equilibrium adsorptions of rhodamine B onto TiO_2/fibre showed the best linearity plot of the correlation coefficient ($R^2 > 0.99$) for both the Langmuir and Freundlich isotherms. The kinetic adsorption obtained from at the different contact time was indicative well pseudo-first- and second-order with correlation coefficient ($R^2 > 0.99$). As a results of this study, nanomaterial TiO_2/fibre can be used as an effective adsorbent for the removal of rhodamine B in aqueous solution.

Acknowledgments: The authors gratefully acknowledge the financial support received from the Faculty Mathematic and Natural Sciences and Director of research and public service of Indonesia Islamic University.

Conflicts of Interest: The authors declare that there is no conflict of interest in this research

References

1. Chen, L.; Lia, Y; Hua, S; Suna, J; Dua, Q; Yanga, X; Jia, Q; Wanga, Z; Wanga, D; Xiaa, Y. Removal of methylene blue from water by cellulose/graphene oxide fibers, Journal of Experimental Nanoscience, 2016, 11, 1156-1170.
2. Kosa, S.A; Al-sebaii, N.M; El Maksod, I.H.A; Hegazy, E.Z. New method for removal of organic dyes using supported iron oxide as a catalyst, Journal of Chemistry, 2016, Article ID 1873175.
3. Suteu, D; Biliuta, G; Rusu, L; Coseri, S; Nacu, G. Cellulose cellets as new type of adsorbent for the removal of dyes from aqueous media, Environmental Engineering and Management Journal; 2015, 14, 525-532.
4. Ajinomoh, C. S; Salahudeen, N. Production of activated carbon from sugar cane bagasse, Australian Society for Commerce Industry & Engineering, 2014.
5. Sugumaran, P; Priya Susan,V; P. Ravichandran; Seshadri, S. Production and characterization of activated carbon from banana empty fruit bunch and delonix regia fruit pod, Journal of Sustainable Energy & Environment 3 (2012) 125-132.
6. Abdul Karim, S.K.; Lim, S.F.; Chua, S.N.D.; Salleh, S.F.; Law, P.L. Banana fibers as sorbent for removal of acid green dye from water, Journal of Chemistry, 2016, 11, 1-11.
7. Khaleque, M.A.; Roy, D.K. Removing reactive dyes from textile effluent using banana fibre, International Journal of Basic & Applied Sciences, 2016, 16, 14-20.
8. Annadurai, G.; Juang, R.S.; Lee, D.J. Adsorption of heavy metals from water using banana and orange peels, Water Science and Technology, 2002, 47, 185-190.
9. Yue, X., Huang, J., Jiang, F., Lin, H., ChenY. Synthesis and characterization of cellulose-based adsorbent for removal of anionic and cationic dyes, Journal of Engineered Fibers and Fabrics, 2019, 14, 1-10.
10. Fard, G.C., Mirjalili1, M., Najafi, F. Preparation of nano-cellulose/A-Fe2O3 hybrid nanofiber for the cationic dyes removal: optimization characterization, kinetic, isotherm and error analysis, Bulgarian Chemical Communications, 2018, 50, 251-261.
11. Moosa, A.A; Ridha, A.M; Kadhim, N.A. Use of biocomposite adsorbents for the removal of methylene blue dye from aqueous solution, American Journal of Materials Science, 2016, 6, 135-146.
12. Jallouli, N., Elghniji, K., Trabelsi, H., Ksibi, M. Photocatalytic degradation of paracetamol on TiO 2 nanoparticles and TiO 2 /cellulosic fiber under UV and sunlight irradiation. Arabian Journal of Chemistry, 2017, 10, S3640–S3645.
13. Tan, M.; Ma, L.; Ur Rahman, M.S.; Ahmed, M.A.; Sajid, M.; Xu, X.; Sun, Y. ; Cui, P.; Xu, J. Screening of acidic and alkaline pretreatments for walnut shell and corn stover biorefining using two way heterogeneity evaluation, Renewable Energy, 2019,132, 950-958.
14. Mopoung, S.; Moonsri, P.; Palas, W.; Khumpai, S. Characterization and properties of activated carbon prepared from tamarind seeds by KOH activation for Fe(III) adsorption from aqueous solution. The Scientific World Journal, 2015, 1–9.
15. Oh, Y. S., Yoo, D II., Shin, Y., Seo, G. FTIR analysis of cellulose treated with sodium hydroxide and carbon dioxide, Carbohydrate Research, 2005, 340, 417-428.
16. Varshney, R.; Bhadauria, S.; Gaur, M.S. Biogenic synthesis of silver nanocubes and nanorods using sundried Stevia rebaudiana leaves. Adv.Mat.Lett. 2010; 1, 232-237.
17. Antic, Z.; Krsmanovic, R.M.; Nikolic, M.G.; Cincovic, M.M.; Mitric, M.; Polizzi, S.; Dramicanin, M.D. Multisite luminescence of rare earth doped TiO2 anatase nanoparticles. Mat.Chem.Phys. 2012; 135: 1064-1069.
18. Zhang, J.; Liu, F.; Gao, J.; Chen, Y.; Hao, X. Ordered mesoporous TiO2/activated carbon for adsorption and photocatalysis of acid red 18 solution, BioRes. 2017. 12, 9086-9102.
19. Ma, Y.; Gao, N.; Chu, W.; Li, C. Removal of phenol by powdered activated carbon adsorption. Frontiers of Environmental Science & Engineering, 2013, 7, 158–165.
20. Weber, W.; Morris, J. Kinetics of adsorption on carbon from solution, Journal of the Sanitary Engineering Division, 1963, 89, 31-60.
21. Singh, S. K; Townsend, T. G.; Macyzk, D.; Boyer, T. H. Equilibrium and intra-particle diffusion of stabilized landfill leachate onto micro- and meso-porous activated carbon, Water Research, 2012, 46, 491-499.

 doi:10.20944/preprints201910.0344.v1

361 22. Panneerselvam, P.; Morad, N.; Tan, K.A.; Mathiyarasi, R. Removal of rhodamine b dye using activated
362 carbon prepared from palm kernel shell and coated with iron oxide nanoparticles. Separation Science and
363 Technology, 2012, 47, 742–752.